Article
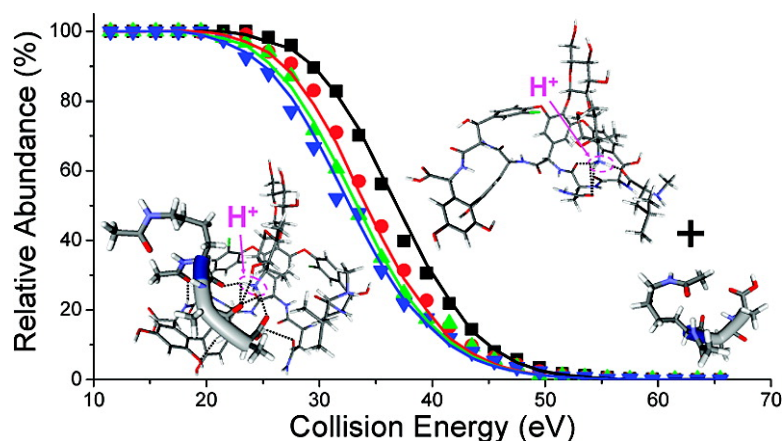
Experimental and Theoretical Studies of the Structures and Interactions of Vancomycin Antibiotics with Cell Wall Analogues

Zhibo Yang, Erich R. Vorpagel, and Julia Laskin

More About This Article

Additional resources and features associated with this article are available within the HTML version:

- Supporting Information
- Access to high resolution figures
- Links to articles and content related to this article
- Copyright permission to reproduce figures and/or text from this article

View the Full Text HTML

Experimental and Theoretical Studies of the Structures and Interactions of Vancomycin Antibiotics with Cell Wall Analogues

Zhibo Yang, Erich R. Vorpagel, and Julia Laskin*

Pacific Northwest National Laboratory, Fundamental Science Directorate, P.O. Box 999 (K8-88), Richland, Washington 99352

Received April 10, 2008; E-mail: Julia.Laskin@pnl.gov

Abstract: Surface-induced dissociation (SID) of the singly protonated complex of vancomycin antibiotic with cell wall peptide analogue (N_α,N_ϵ-diacetyl-L-Lys-D-Ala-D-Ala) was studied using a 6 T Fourier Transform Ion Cyclotron Resonance Mass Spectrometer (FT-ICR MS) specially configured for SID experiments. The binding energy between the vancomycin and the peptide was obtained from the RRKM modeling of the time- and energy-resolved fragmentation efficiency curves (TFECs) of the precursor ion and its fragments. Molecular dynamics simulations of the vancomycin, peptide, and vancomycin-peptide complex were carried out to explore the low energy conformations. Density functional theory (DFT) calculations of the geometries, proton affinities, and binding energies were performed for several model systems including vancomycin (V), vancomycin aglycon (VA), N_α,N_ϵ-diacetyl-L-Lys-D-Ala-D-Ala, and noncovalent complexes of VA with N-acetyl-D-Ala-D-Ala and V with N_α,N_ϵ-diacetyl-L-Lys-D-Ala-D-Ala. Comparison between the experimental and computational results suggests that the most probable structure of the complex observed in our experiments corresponds to the neutral peptide bound to the vancomycin protonated at the primary amine of the disaccharide group. The experimental binding energy of 30.9 ± 1.8 kcal/mol is in good agreement with the binding energy of 36.3−42.0 kcal/mol calculated for the model system representing the preferred structure of the complex.

1. Introduction

Vancomycin (V, Figure 1) is a glycopeptide antibiotic that is widely used for treatment of infections caused by Gram-positive bacterial pathogens.[1] It is a tricyclic molecule that contains the L-vancosaminyl-α(1→2)-D-glucopyranosyl disaccharide group (R$_1$ = disaccharide); N-methyl-leucine in position 1 (R$_2$ = CH$_3$); substituted phenylglycines in positions 2, 4, 5, 6, and 7; and asparagine in position 3.[2] Detailed understanding of the mechanism of action of glycopeptide antibiotics is important for the development of new agents necessary to overcome the emerging bacterial resistance to vancomycin. It is known that vancomycin prevents the growth of the bacterial cell wall by binding to the cell-wall peptidoglycan precursors terminating in -L-Lys-D-Ala-D-Ala.[1–4] Molecular recognition between vancomycin and -D-Ala-D-Ala containing peptide ligands has been extensively investigated using a variety of experimental techniques, making the vancomycin−peptide

complex an ideal model system for the development of new approaches for understanding biomolecular recognition processes.[2–10] N-acetyl-D-Ala-D-Ala (AcDADA) and N_α,N_ϵ-diacetyl-L-Lys-D-Ala-D-Ala (Ac$_2$KDADA) shown in Figure 2 are commonly used to mimic cell-wall receptors.

Previous studies examined the role of different vancomycin subunits in the molecular interactions important for the bacterial cell-wall peptide analogue recognition.[1,2,7,11] It has been demonstrated that, for example, substitution of one of the two chlorine atoms with hydrogen reduces the antibiotic-peptide affinity by a factor of 2,[12] whereas replacement of the N-methyl-leucine with leucine (R$_2$ = H) increases the antibiotic activity against both *Staphylococcus aureus* and methicillin resistant *S. aureus*.[13] While the disaccharide unit is not directly involved in the binding of the ligand, it plays an important role in

(1) (a) Nieto, M.; Perkins, H. R. *Biochem. J.* **1971**, *123*, 773. (b) Anderson, J. S.; Matsuhashi, M.; Haskin, M. A.; Strominger, J. L. *Proc. Natl. Acad. Sci. U.S.A.* **1965**, *53*, 881. (c) Anderson, J. S.; Matsuhashi, M.; Haskin, M. A.; Strominger, J. L. *J. Bio. Chem.* **1967**, *242*, 3180. (d) Reynolds, P. E. *Biochim. Biophys. Acta* **1961**, *52*, 403. (e) Reynolds, P. E. *Symp. Soc. Gen. Microbiol.* **1966**, *16*, 47.
(2) Loll, P. J.; Axelsen, P. H. *Annu. Rev. Biophys. Biomol. Struc.* **2000**, *29*, 265.
(3) (a) Willianms, D. H.; Bardsley, B. *Angew. Chem., Int. Ed.* **1999**, *38*, 1172. (b) Perkins, H. R. *Biochem. J.* **1969**, *111*, 195.
(4) (a) Vollmerhaus, P. J.; Breukink, E.; Heck, A. J. R. *Chem.−Eur. J.* **2003**, *9*, 1556. (b) Chatterjee, An. N.; Perkins, H. R. *Biophys. Res. Commun.* **1966**, *24*, 489.
(5) Williams, D. H.; Stephens, E.; O'Brien, D. P.; Zhou, M. *Angew. Chem., Int. Ed.* **2004**, *43*, 6596.
(6) Lim, H.-K.; Hsieh, Y.; Ganem, B.; Henion, J. *J. Mass. Spectrom.* **1995**, *30*, 708.
(7) Jørgensen, T. J. D.; Staroske, T.; Roepstorff, P.; Williams, D. H.; Heck, A. J. R. *J. Chem. Soc., Perkin Trans. 2* **1999**, 1859.
(8) Vollmerhaus, P. J.; Tempels, F. W. A.; Kettenes-van den Bosch, J. J.; Heck, A. J. R. *Electrophoresis* **2002**, *23*, 868.
(9) Jusuf, S.; Loll, P. J.; Axelsen, P. H. *J. Am. Chem. Soc.* **2003**, *125*, 3988.
(10) Heck, A. J. R.; Jørgensen, T. J. D. *Int. J. Mass Spectrom.* **2004**, *236*, 11.
(11) Gerhard, U.; Mackay, J. P.; Maplestone, R. A.; Williams, D. H. *J. Am. Chem. Soc.* **1993**, *115*, 232.
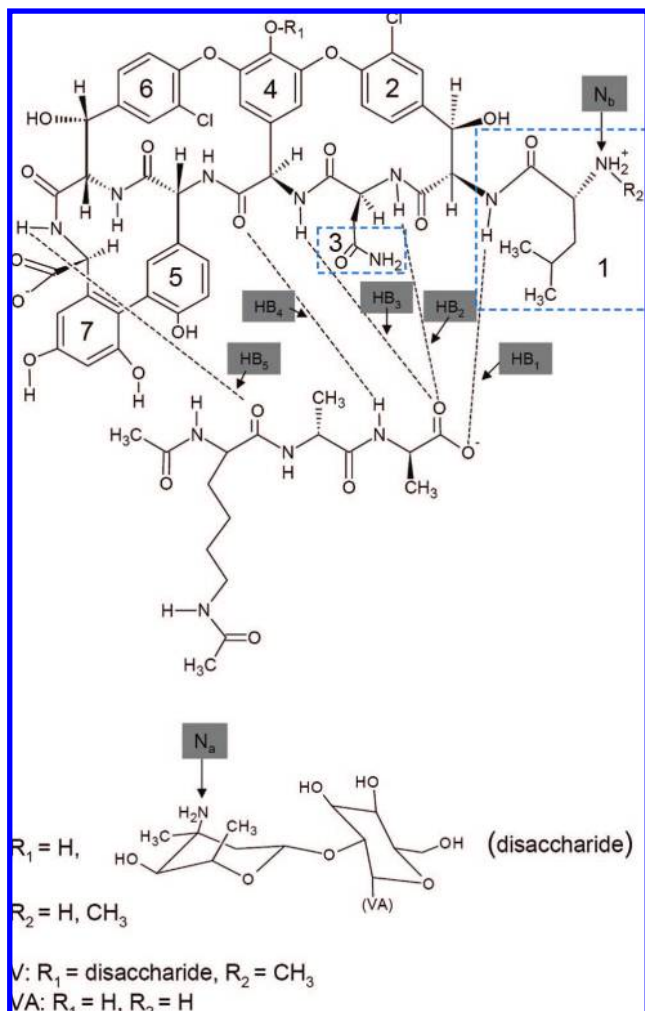(12) Harris, C. M.; Kannan, R.; Kopecka, H.; Harris, T. M. *J. Am. Chem. Soc.* **1985**, *107*, 6652.

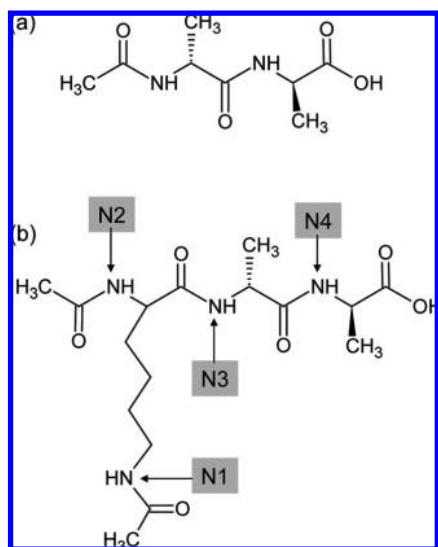**Figure 1.** Schematic structure of the V−Ac₂KDADA complexes in solution.

Figure 2. Schematic structures of (a) *N*-acetyl-D-Ala-D-Ala (AcDADA) and (b) N_α,N_ϵ-diacetyl-L-Lys-D-Ala-D-Ala (Ac₂KDADA) with indication of protonation sites.

binding.[11,14] Removing this group decreases the antibiotic potency of vancomycin and reduces its solubility in water.[15]

Detailed NMR investigations addressed the molecular basis of the interaction between vancomycin and the cell wall using V−AcDADA and V−Ac₂KDADA complexes as model systems.[16−19] It has been demonstrated that in solution the disaccharide group of vancomycin (R_1, Figure 1) is protonated whereas the vancomycin cage exists as the zwitterionic structure, in which the deprotonated C-terminus and the protonated N-terminus are stabilized by the solvent. The schematic structure of V−Ac₂KDADA in solution showing all possible hydrogen bonding interactions is presented in Figure 1. NMR experiments indicate that five hydrogen bonds are formed between vancomycin and the peptide ligand in the complex: three of them (HB_1, HB_2, and HB_3) involve the deprotonated C-terminus of the peptide solvated by three amide-NH groups of vancomycin, and the other two (HB_4 and HB_5) are formed between the backbone amide and carbonyl groups of the peptide and vancomycin. The acetylated N-terminus of the peptide and the lysine side chain are exposed to the solvent and are not involved in the intermolecular hydrogen bonding interaction.

It has been demonstrated that the equilibrium binding constant between vancomycin and Ac₂KDADA depends on the pH and the composition of the solution,[1,20] suggesting that for this system the experimental determination of the binding affinity is influenced by the properties of the solvent. In contrast, gas-phase experiments provide a unique opportunity to study the intrinsic properties of noncovalent complexes in the absence of solvent. However, the solution-phase structures are not necessarily preserved in the gas phase. It has been demonstrated that small peptides undergo substantial conformational change in the gas-phase[21,22] while proteins and noncovalent protein complexes retain much of their solution-phase structure.[23,24] Jørgensen et al.[25] examined the relative stability of noncovalent complexes of vancomycin with cell wall analog peptides in the gas phase using collision-induced dissociation (CID) experiments. They found that the relative stabilities of doubly deprotonated complexes toward fragmentation determined from the experimental appearance energies of the product ions were correlated with the corresponding association constants in solution, while the stabilities of doubly protonated complexes were independent of the peptide ligand. They suggested that the original solution-phase structure of vancomycin responsible for selective binding of D-Ala-D-Ala peptides was preserved only in the negative mode.

(13) Yao, N. H.; Liu, G.; He, W. Y.; Niu, C. Q.; Carlson, J. R.; Lam, K. S. *Bioorg. Med. Chem. Lett.* **2005**, *15*, 2325.
(14) Kaplan, J.; Korty, B. D.; Axelsen, P. H.; Loll, P. J. T. *J. Med. Chem.* **2001**, *44*, 1837.
(15) Kannan, R.; Harris, C. M.; Harris, T. M.; Waltho, J. P.; Skelton, N. J.; Williams, D. H. *J. Am. Chem. Soc.* **1988**, *110*, 2946.
(16) Williamson, M. P.; Williams, D. H. *J. Am. Chem. Soc.* **1981**, *103*, 6580.
(17) Williams, D. H.; Williamson, M. P.; Butcher, D. W.; Hammond, S. J. *J. Am. Chem. Soc.* **1983**, *105*, 1332.
(18) Williams, D. H. *Acc. Chem. Res.* **1984**, *17*, 364.
(19) Yao, N. H.; He, W. Y.; Lam, K. S.; Liu, G. *J. Comb. Chem.* **2005**, *7*, 123.
(20) Popieniek, P. H.; Pratt, R. F. *J. Am. Chem. Soc.* **1991**, *113*, 2264.
(21) Jarrold, M. F. *Annu. Rev. Phys. Chem.* **2000**, *51*, 179.
(22) Wyttenbach, T.; Liu, D.; Bowers, M. T. *Int. J. Mass Spectrom.* **2005**, *240*, 221.
(23) Loo, J. *Int. J. Mass Spectrom.* **2000**, *200*, 175.
(24) Hoaglund-Hyzer, C. S.; Counterman, A. E.; Clemmer, D. E. *Chem. Rev.* **1999**, *99*, 3037.
(25) Jørgensen, T. J. D.; Delforge, D.; Remacle, J.; Bojesen, G.; Roepstorff, P. *Int. J. Mass Spectrom.* **1999**, *188*, 63.

determining the antibiotic activity of vancomycin by enhancing dimerization of and contributing to the cooperativity of ligand

Appearance energy determinations discussed earlier provide interesting qualitative information on the relative stability of gas-phase ions toward fragmentation. The stability of gas-phase ions is determined both by the threshold energy and by the activation entropy of dissociation that cannot be distinguished based on the appearance energy measurements alone.[26] Our previous studies demonstrated that SID combined with the long and variable time scale of a Fourier transform ion cyclotron resonance mass spectrometer (FT-ICR MS) is perfectly suited for studying the energetics and dynamics of the gas-phase fragmentation of peptide ions.[26–28] Time- and collision-energy resolved studies provide important information both on the appearance energies and the kinetics of formation of different fragment ions. RRKM-based modeling of the experimental data developed by our group[29,30] enables accurate determination of threshold energies and activation entropies for different dissociation channels of complex precursor ions. The modeling approach was initially tested by studying fragmentation of polyatomic molecules with well-known fragmentation energetics and was subsequently used to determine the energetics and dynamics of dissociation of a variety of peptide ions.[26–28] Here we present the first study focused on the determination of energy and entropy effects in dissociation of noncovalent complexes using time- and energy-resolved SID experiments.

The binding affinity between vancomycin and -D-Ala-D-Ala containing peptides has been extensively studied using both theoretical calculations[31,32] and solution-phase experimental measurements.[7,33–35] Because in solution the disaccharide group of vancomycin does not directly participate in the binding, vancomycin aglycon (VA), the vancomycin analog without the disaccharide group, is commonly used as a model system in computational studies. Hartree-Forck (HF/6−31G(d)) and density functional theory (B3LYP/6−31G(d)) calculations were performed to examine gas phase binding affinity of the deprotonated AcDADA ([AcDADA − H]$^-$) with the protonated VA ([VA + H]$^+$), in which both R_1 and R_2 were replaced with hydrogen atoms.[31,32] The qualitative trends in calculated affinities of VA with different peptide ligands were consistent with the trends in the experimental dissociation constants. However, no direct comparison between the theoretical and experimental binding energies in such systems has been reported so far.

In this work we present a combined experimental and theoretical study of the gas-phase stability of the singly protonated V−Ac$_2$KDADA complex. Time- and energy-resolved SID experiments were performed using a specially designed FT-

ICR MS configured for studying ion-surface collisions.[36] The energetics and dynamics of dissociation were determined using the RRKM modeling of the experimental data. The results are compared with the density functional theory (DFT) calculations for a number of model systems including VA, V, cell-wall peptide analogues (AcDADA and Ac$_2$KDADA), and noncovalent complexes of VA with AcDADA and V with Ac$_2$KDADA. We present first direct comparison between the experiment and theory for the vancomycin-peptide model system, and demonstrate that combination of SID experiments and theoretical calculations is an effective approach for obtaining molecular-level understanding of noncovalent interactions in biomolecular systems.

2. Experimental Section

SID experiments were conducted using a specially fabricated 6T FT-ICR mass spectrometer described in detail elsewhere.[36] The instrument is equipped with an external electrospray ionization source consisting of an ion funnel[37] followed by three quadrupoles. Ions exiting the ion funnel undergo collisional relaxation and focusing in the first collisional quadrupole prior to transfer into a mass-resolving quadrupole. Mass selected ions are efficiently thermalized in the accumulation quadrupole, which removes internal and translational energy originating from the ion source and ion funnel. After accumulation, ions are extracted from the third quadrupole and transferred into the ICR cell where they collide with the surface. Scattered ions are captured by raising the potentials on the front and rear trapping plates of the ICR cell by 10−20 V. Immediately following the reaction delay, ions were excited by a broadband chirp and detected. The collision energy is defined by the difference between the dc offset of the accumulation quadrupole and the potential applied to the rear trapping plate of the ICR cell and the SID target. The ICR cell can be offset above or below ground by as much as ±150 V. Lowering the ICR cell below ground while keeping the potential on the third quadrupole fixed increases collision energy for positive ions. Data acquisition was accomplished with a MIDAS data station developed by Marshall and co-workers at the National High Magnetic Field Laboratory.[38]

Time-resolved spectra were obtained by varying the delay between the gated trapping and the excitation/detection event (the reaction delay). Experiment involved changing the collision energy across a relatively wide range from 11.5 to 65.5 eV in 2 eV increments for four reaction delay times of 1, 5, 10, and 50 ms. The precursor ions survival curves (SCs) and time-resolved fragmentation efficiency curves (TFECs) were constructed from experimental mass spectra by plotting the relative abundance of the precursor ion and its fragments as a function of collision energy for each reaction delay.

Self-assembled monolayers of alkyl thiols (HSAM) were prepared on a on a single gold {111} crystal (Monocrystals, Richmond Heights, OH) using a standard procedure. Prior to SAM deposition, the gold surface was cleaned using a UV cleaner (Boekel Industries Inc., model 135500) for 10 min, and then immersed for at least 12 h in a 1 mM ethanol solution of the 1-dodecanethiol, CH$_3$(CH$_2$)$_{11}$SH, (Sigma-Aldrich, St. Louis, MO). Extra layers of the HSAM were removed by ultrasonic cleaning in ethanol for 10 min prior to the experiment.

Vancomycin hydrochloride and Ac$_2$KDADA were purchased from Sigma-Aldrich (St. Louis, MO). The samples were dissolved in 50:50 (*v/v*) methanol:water solution to a final concentration of vancomycin:Ac$_2$KDADA about 300:50 μM. A syringe pump (Cole

(26) Laskin J. Energy and Entropy Effects in Gas-Phase Dissociation of Peptides and Proteins. In Principles of Mass Spectrometry Applied to Biomolecules. In *Principles of Mass Spectrometry Applied to Biomolecules*; Laskin, J., Lifshitz, C., Eds.; John Wiley & Sons: New York, 2006.

(27) Laskin, J.; Denisov, E.; Futrell, J. *J. Am. Chem. Soc.* **2000**, *122*, 9703.

(28) Laskin, J. *Eur. J. Mass Spectrom* **2004**, *10*, 259.

(29) Laskin, J.; Byrd, M.; Futrell, J. *Int. J. Mass Spectrom.* **2000**, *195*, 285.

(30) Laskin, J.; Futrell, J. *J. Phys. Chem. A* **2000**, *104*, 5484.

(31) Lee, J. G.; Sagui, C.; Roland, C. *J. Phys. Chem. B* **2005**, *109*, 20588.

(32) Lee, J. G.; Sagui, C.; Roland, C. *J. Am. Chem. Soc.* **2004**, *126*, 8384.

(33) Rekharsky, M.; Hesek, D.; Lee, M.; Meroueh, S. O.; Inoue, Y.; Mobashery, S. *J. Am. Chem. Soc.* **2006**, *128*, 7736.

(34) Williamson, M. P.; Williams, D. H.; Hammond, S. J. *Tetrahedron* **1984**, *40*, 569.

(35) Jørgensen, T. J. D.; Roepstorff, P.; Heck, A. J. R. *Anal. Chem.* **1998**, *70*, 4427.

(36) Laskin, J.; Denisov, E. V.; Shukla, A. K.; Barlow, S. E.; Futrell, J. H. *Anal. Chem.* **2002**, *74*, 3255.

(37) Shaffer, S. A.; Tang, K. Q.; Anderson, G. A.; Prior, D. C.; Udseth, H. R.; Smith, R. D. *Rapid Commun. Mass Spectrom.* **1997**, *11*, 1813.

(38) Senko, M. W.; Canterbury, J. D.; Guan, S.; Marshall, A. G. *Rapid Commun. Mass Spectrom.* **1996**, *10*, 1839.

Scheme 1
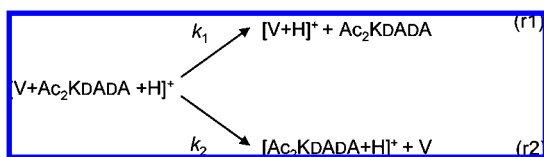
Parner, Vernon Hills, IL) was used for direct infusion of the electrospray sample at a flow rate of 25 μL/h.

3. RRKM Modeling

TFECs were modeled using an RRKM-based approach developed by our group.[29,30] Energy-dependent microcanonical rate constants for the total decomposition of the precursor ion, $k(E)$, were calculated using the RRKM/QET expression:

$$k(E) = \frac{\sigma W^{\ddagger}(E - E_0)}{\hbar \rho(E)} \quad (1)$$

where $\rho(E)$ is the density states of the reactant, $W^{\ddagger}(E - E_0)$ is the sum of states of the transition state, E_0 is the threshold energy, $\hbar$ is Planck's constant, and σ is the reaction path degeneracy.

Relative abundance of the precursor ion and its fragments as a function of the internal energy and the experimental observation time (t_r), $F_i(E, t_r)$, was calculated taking into account the radiative cooling of the vibrationally excited ion. The energy deposition function (EDF) was described by the following analytical expression[29,30]

$$P(E, E_{coll}) = \frac{1}{C}(E - \Delta)^l \exp\left(-\frac{(E - \Delta)}{f(E_{coll})}\right) \quad (2)$$

where $C = \Gamma(l + 1)[f(E_{coll})]^{l+1}$ is a normalization factor, l and Δ are parameters, and $f(E_{coll})$ has the form:

$$f(E_{coll}) = A_2 E_{coll}^2 + A_1 E_{coll} + A_0 \quad (3)$$

where A_0, A_1, and A_2 are parameters, and E_{coll} is the collision energy.

Finally, the normalized abundance of the precursor or a fragment ion for each collision energy, $I_i(E_{coll})$, and reaction time, t_r, was calculated using the following expression:

$$I_i(E_{coll}) = \int_0^{\infty} F_i(E, t_r)P(E, E_{coll})dE \quad (4)$$

Gas-phase fragmentation of the singly protonated vancomycin-Ac_2KDADA complex ($[V + Ac_2KDADA + H]^+$), follows two major dissociation pathways (r1 and r2) shown in Scheme 1. Reaction r1 results in formation of the protonated vancomycin ($[V + H]^+$) and neutral peptide, while neutral vancomycin, V, and protonated Ac_2KDADA ($[Ac_2KDADA + H]^+$) are products of reaction r2. The breakdown graph for $[V + Ac_2KDADA + H]^+$ and its fragments was constructed using the two-decay rate model that takes into account the radiative decay of the precursor ion. Radiative decay rate was assumed to be independent of the internal energy. This approximation is justified because radiative rates exhibit a very slow dependence on the internal energy of the ion as compared to fragmentation rates.[39]

Calculated TFECs were constructed using the above procedure and compared with the experimental data. The EDF was kept the same for all reaction times. The fitting parameters were varied until the best fit to experimental curves was obtained.

The fitting parameters included critical energies and the activation entropies for the two reaction channels, the rate constant for the radiative decay, k_{rad}, and the parameters characterizing the EDF (eqs 2 and 3). The uniqueness of the fits was confirmed using the sensitivity analysis described previously.[29,30]

Vibrational frequencies of the precursor ion were obtained from the theoretical calculations described below. Vibrational frequencies for the transition state were estimated by removing one vibrational mode (reaction coordinate, which is assumed to be 1000 cm^{-1}) from the precursor ion frequencies and scaling all frequencies in the range of 500−1000 cm^{-1} as a group to obtain the best fit with the experimental data.

4. Theoretical Calculations

Molecular modeling was performed on an SGI Onyx 3200 workstation running Insight II/Discover (97.0, Accelrys Software Inc., San Diego, CA). The original structure of vancomycin obtained from protein data bank (PDB) was used as the reference.[40] Preliminary structures of the neutral and protonated species of peptide (Ac_2KDADA and $[Ac_2KDADA + H]^+$), vancomycin (V and $[V + H]^+$), and singly protonated vancomycin-peptide model complexes ($[V + Ac_2KDADA + H]^+$) were built using the Biopolymer builder of Insight II. Both initial and final structures of the vancomycin and vancomycin-peptide complexes were energy minimized using the CFF91 force field.[41] Because of the absence of the CFF91[41] force field for protonated amide ($-CONH_2^+-$) in the Insight II software package, energy minimization of both Ac_2KDADA and $[Ac_2KDADA + H]^+$ were carried out using the Amber force field.[42] All the minimizations were performed using quasi-Newton−Raphson (VA09A) algorithm.[43] Conformational space of complex ions and neutral molecules was explored using molecular dynamics (MD) simulations performed at 1000 K for monomers (V, $[V + H]^+$, Ac_2KDADA, and $[Ac_2KDADA + H]^+$) and 500 K for complexes ($[V + Ac_2KDADA + H]^+$) in vacuum with a 1.0 fs time step. Conformations were saved at 2 ps intervals over a 1 ns dynamics run. Each structure was then minimized and the lowest energy structure of each species was chosen for DFT calculations.

DFT calculations were carried out using NWChem (version 5.0) developed and distributed by the Pacific Northwest National Laboratory (PNNL).[44] Extensible Computational Chemistry Environment (ECCE) developed at PNNL[45] was used to setup calculations and visualize the results. Preliminary geometry optimization was performed at the B3LYP/3−21G level of theory. Final geometries, single-point energies, as well as vibrational frequencies of Ac_2KDADA and $[Ac_2KDADA + H]^+$ were obtained by subsequent optimization and frequency analyses of these structures at the B3LYP/6−31G(d) level of theory. The hybrid computational method (ONIOM) was used for the structure optimization and single-point energy calculation for $[V + H]^+$ and $[V + Ac_2KDADA + H]^+$, where B3LYP/6−31G(d) was applied to Ac_2KDADA and the atoms related to the hydrogen bonding between $[V + H]^+$ and $[V + Ac_2KDADA + H]^+$, and B3LYP/3−21G was applied to the

(39) Dunbar, R. C. *Mass Spectrom. Rev.* **1992**, *11*, 309.

(40) (a) http://www.rcsb.org, and PDB code is 1aa5. (b) Loll, P. J.; Bevivino, A. E.; Korty, B. D.; Axelen, P. H. *J. Am. Chem. Soc.* **1997**, *119*, 1516.

(41) Maple, J.; Dinur, U.; Hagler, A. T. *Proc. Natl. Acad. Sci. U.S.A.* **1988**, *85*, 5350.
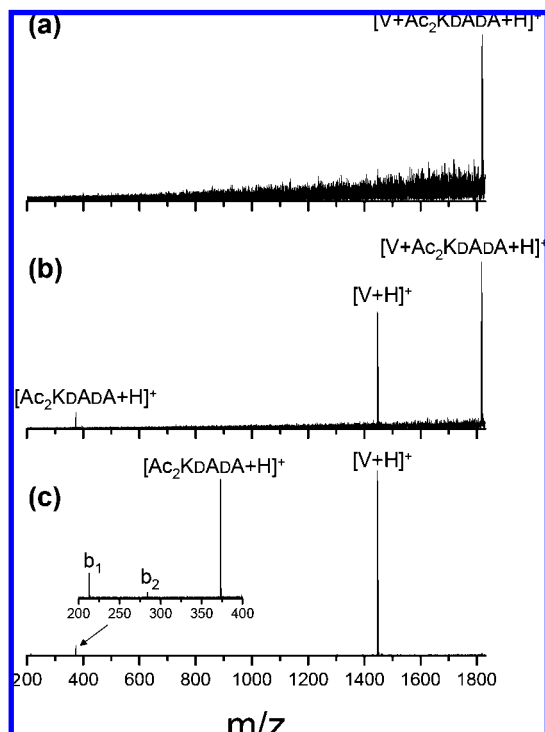
(42) Weiner, S. J.; Kollman, P. A.; Nguyen, D. T.; Case, D. A. *J. Comput. Chem.* **1986**, *7*, 230.

(43) Powell, M. J. D. *Math. Program.* **1977**, *12*, 241.

(44) Bylaska, E. J. *NWChem, A Computational Chemistry Package for Parallel Computers, Version 5.1*; Pacific Northwest National Laboratory: Richland, WA, 2007.

(45) Black, G. *Ecce, A Problem Solving Environment for Computational Chemistry, Software Version 4.0.1*; Pacific Northwest National Laboratory: Richland, WA, 2006.

Figure 3. SID spectra of $[V + Ac_2K_DAD_A + H]^+$ at collision energies of (a) 19.5, (b) 35.5, and (c) 55.5 eV. The insert in (c) shows consecutive fragmentation products of $[Ac_2K_DAD_A + H]^+$.

rest of the atoms.[46] Harmonic vibrational frequencies of $[V + H]^+$ and $[V + Ac_2K_DAD_A + H]^+$ were calculated using ONIOM and B3LYP/3−21G methods, respectively. Calculated vibrational frequencies of the model systems were used to obtain zero-point energy (ZPE) corrections and utilized in the RRKM modeling of the experimental data. Binding energies were determined based on single-point energies of the model systems simulating precursor complexes and their products and included the ZPE correction.

5. Results

5.1. SID Spectra. Figure 3 shows SID spectra of $[V + Ac_2K_DAD_A + H]^+$ obtained at collision energies of 19.5, 35.5, and 55.5 eV and 1 ms fragmentation delay. No fragmentation is observed at this reaction delay for collision energies below 19.5 eV, while at 35.5 eV about 50% of the precursor ions undergo fragmentation. Two competitive product ions are observed in the 35.5 eV SID spectrum corresponding to the major protonated vancomycin fragment, $[V + H]^+$, and the minor peptide fragment, $[Ac_2K_DAD_A + H]^+$. At collision energies above 55.5 eV the precursor ion is completely fragmented, and the dominant product is the $[V + H]^+$ ion. The relative abundance of the $[Ac_2K_DAD_A + H]^+$ is less than 3% in the entire range of experimental collisional energies;[47] small amount of its subsequent fragments (b_1 and b_2) is observed at collision energies above 55.5 eV. In addition, four minor (<7%) fragments of vancomycin ($[V + H − 143]^+$, $[V + H − 305]^+$, $[V + H − 1036]^+$ and $[V + H − 1052]^+$) were observed at collision energies above 57.5 eV.

(46) The atoms and corresponding levels of theory applied in the calculations of V, $[V + H]^+$, and $[V + Ac_2K_DAD_A + H]^+$ are detailed in the Supporting Information.
(47) The relative abundance of the precursor ion and its fragments was determined by summing up all the isotopic peaks.
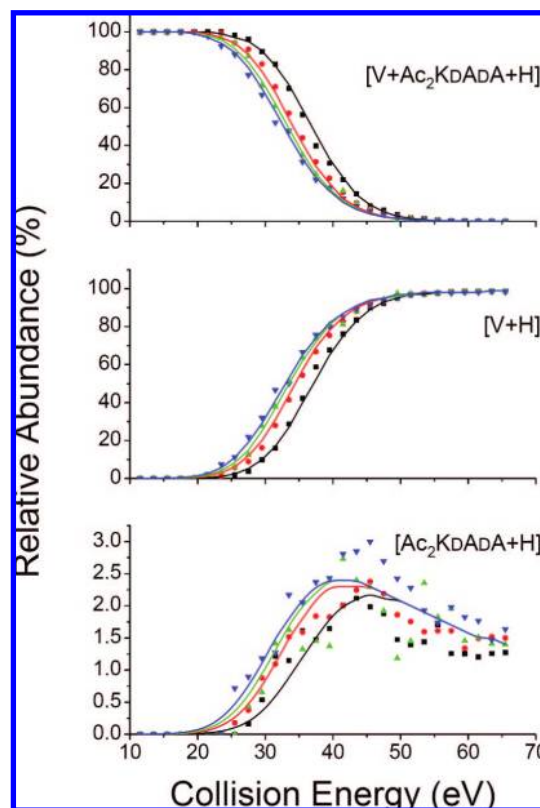
Figure 4. Experimental TFECs for (a) precursor ion $[V + Ac_2K_DAD_A + H]^+$, (b) major product $[V + H]^+$, and (c) minor product $[Ac_2K_DAD_A + H]^+$ for reaction delays of 1 ms (■), 5 ms (•), 10 ms (▲), and 50 ms (▼). The solid lines show the results of the RRKM modeling.

5.2. Time-Resolved Studies. Time-resolved survival curves (SCs) for the precursor ion and fragmentation efficiency curves (TFECs) of its fragments were obtained by varying the collision energy and the reaction time and plotting the relative abundance of each ion as a function of collision energy for each fragmentation delay. SCs and TFECs of the $[V + Ac_2K_DAD_A + H]^+$, $[V + H]^+$, and $[Ac_2K_DAD_A + H]^+$ ions are shown in Figure 4 (symbols). SCs of the precursor ion and TFECs of fragments exhibit fairly weak dependence on the reaction time. For example, increasing the reaction delay from 1 to 50 ms results in a 4.5 eV decrease in the collision energy at which 50% of the $[V + Ac_2K_DAD_A + H]^+$ ion has decomposed ($E_{50\%}$). This should be compared with the collision energy shift of ca. 22 eV reported previously for SID of the singly protonated des-Arg[1]-bradykinin ($[PPGFSPFR + H]^+$)—a much smaller ion than $[V + Ac_2K_DAD_A + H]^+$—on the HSAM surface.[48] Our previous studies demonstrated that kinetically hindered fragmentation associated with negative values of activation entropy shows dramatic decrease in $E_{50\%}$ as a function of reaction time while kinetically favored fragmentation is characterized by much smaller decrease in the value of $E_{50\%}$.[49,50] Furthermore, because microcanonical rate constants decrease rapidly with increase in the size of the system, more significant time dependence of TFECs is anticipated for larger ions. Fairly weak time dependence observed for the $[V + Ac_2K_DAD_A + H]^+$ complex as

(48) Laskin, J.; Futrell, J. H. *J. Chem. Phys.* **2003**, *119*, 3413.
(49) Bailey, T. H.; Laskin, J.; Futrell, J. H. *Int. J. Mass Spectrom.* **2003**, *222*, 313.
(50) Laskin, J.; Bailey, T. H.; Futrell, J. H. *Int. J. Mass Spectrom.* **2004**, *234*, 89.

Table 1. Threshold energies and 450 K activation entropies for dissociation channels r_1 and r_2 obtained from experimental data fitting

|	k_1	k_2
E_0, eV	1.34 ± 0.08	1.32 ± 0.08
$\Delta S^{\ddagger, a}$ e.u.	79.3 ± 3.6	62.1 ± 4.2
$A,^b$ s^{-1}	5.5×10^{30}	9.4×10^{26}

^{a} Entropy units (e.u.) = cal (mol•K)$^{-1}$. ^{b} Calculated from $\Delta S^{\ddagger}$ assuming a temperature of 450 K.

compared to a much smaller [PPGFSPFR + H]$^+$ system suggests that gas-phase fragmentation of this complex follows entropically favored pathways. Because of the low relative abundance of the [Ac$_2$K$_D$A$_D$A + H]$^+$ fragment ion, its TFECs show a significant scatter.

5.3. RRKM Modeling. RRKM modeling described earlier was utilized to determine the energetics and dynamics of the gas-phase fragmentation of [V + Ac$_2$K$_D$A$_D$A + H]$^+$. Modeling results were obtained by simultaneously fitting the SCs of the precursor ion and the TFECs of the primary fragments, [V + H]$^+$ and [Ac$_2$K$_D$A$_D$A + H]$^+$. For simplicity, the relative abundance of the secondary fragments was added to the relative abundance of the corresponding primary products. The fitting results are shown as solid lines in Figure 4, and the corresponding dissociation parameters are summarized in Table 1. The model reproduces very well the experimental curves of the precursor ion and its major fragment, [V + H]$^+$ and provides a reasonable representation of the major trends in the experimental TFECs for the minor [Ac$_2$K$_D$A$_D$A + H]$^+$ fragment ion. Both reaction channels are characterized by very similar threshold energies of 1.34 and 1.32 eV for reactions r1 and r2, respectively, while activation entropies, $\Delta S^{\ddagger}$, for reactions r1 (79.3 ± 3.6 e.u.) and r2 (62.1 ± 4.2 e.u.) are quite different, indicating that formation of the protonated vancomycin and the neutral peptide is entropically more favorable than formation of the neutral vancomycin and the protonated peptide. The calculated Arrhenius pre-exponential factor for r1 (5.5 × 10^{30} s^{-1}) is more than 3 orders of magnitude higher than the pre-exponential factor obtained for r2 (9.4 × 10^{26} s^{-1}), suggesting that the microcanonical rate constant for reaction r1 increases much faster with the internal energy of the protonated precursor ion than the rate constant of the formation of the [Ac$_2$K$_D$A$_D$A + H]$^+$ product ion.

5.4. Theoretical Calculations. Very large values of activation entropies for both dissociation pathways obtained from the RRKM modeling (Table 1) indicate that both reactions r1 and r2 proceed via loose transition states without significant reverse activation barriers. It follows that the energetics of these reactions can be adequately described using single-point energy calculations for the optimized structures of the reactant and the products. Density functional theory (DFT) calculations were performed to determine proton affinities (PAs) of vancomycin and Ac$_2$K$_D$A$_D$A and possible structures of V–Ac$_2$K$_D$A$_D$A complexes in the gas phase. The binding affinities for all model systems were derived from the relative energies of the V–Ac$_2$K$_D$A$_D$A complexes and the major products (e.g., the model structures simulating protonated vancomycin and the neutral peptide). Vibrational frequency calculations were performed to determine the zero-point energy (ZPE) corrections for the PAs of Ac$_2$K$_D$A$_D$A and V and the binding energy of [V + Ac$_2$K$_D$A$_D$A + H]$^+$.

5.4.1. Structures and Energetics of [V + Ac$_2$K$_D$A$_D$A + H]$^+$. MD simulations performed for a variety of possible
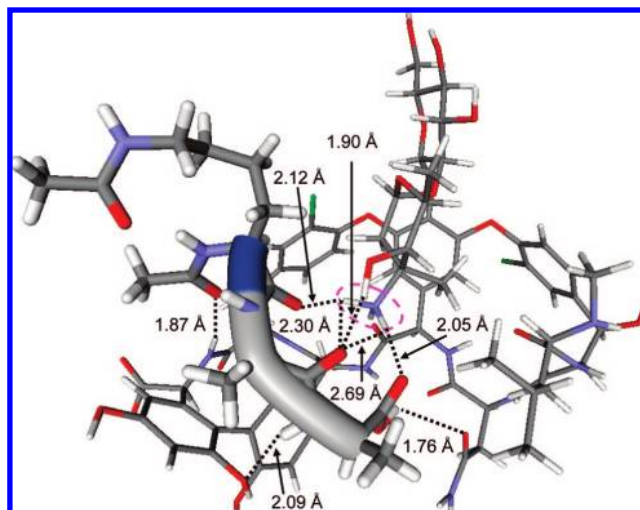
Figure 5. ONIOM(B3LYP/6−31G(d):B3LYP/3−21G) optimized structures of [V + Ac$_2$K$_D$A$_D$A + H]. The thin lines indicate [V + H]$^+$, the thick sticks indicate Ac$_2$K$_D$A$_D$A with the backbone shown as a tube, the dotted lines indicate the intermolecular hydrogen bonds between [V + H]$^+$ and Ac$_2$K$_D$A$_D$A, and the pink dash encloses the protonation site.

structures of [V + H]$^+$ ions demonstrated that structures protonated at the disaccharide group of vancomycin (N$_a$) are more stable than the corresponding structures protonated at the N-methyl leucine (N$_b$) by about 49−50 kcal/mol for [V + Ac$_2$K$_D$A$_D$A + H]$^+$ and 40−43 kcal/mol for [V + H]$^+$. It follows that both the reactant ([V + Ac$_2$K$_D$A$_D$A + H]$^+$) and the major product ([V + H]$^+$) observed in our experiments are most likely protonated at the N$_a$ site. Analysis of the low-energy MD structures of the [V + Ac$_2$K$_D$A$_D$A + H]$^+$ model complex protonated at N$_a$ indicate that the ionizing proton is involved in the intermolecular hydrogen bonding between the vancomycin and the Ac$_2$K$_D$A$_D$A. Due to the limited computational resources, only the lowest energy structure of the [V + Ac$_2$K$_D$A$_D$A + H]$^+$ model complex obtained from MD simulations was selected for subsequent minimization using DFT. The optimized structure obtained using ONIOM (B3LYP/6−31G(d):B3LYP/3−21G) calculations is shown in Figure 5. In this structure, the protonated N$_a$ is solvated by the carbonyl and carboxyl groups of the Ac$_2$K$_D$A$_D$A via four intermolecular hydrogen bonds (2.05−2.69 Å). In addition, one of the hydroxyl groups of the disaccharide moiety and three functional groups of the vancomycin cage (one carbonyl, one hydroxyl, and one secondary amine) form four strong hydrogen bonds (1.76−2.09 Å) with the carbonyl and hydroxyl groups of the Ac$_2$K$_D$A$_D$A.

5.4.2. [V + Ac$_2$K$_D$A$_D$A + H]$^+$ Binding Affinity. As discussed previously, gas-phase fragmentation of the [V + Ac$_2$K$_D$A$_D$A + H]$^+$ complex is dominated by the formation of [V + H]$^+$ and Ac$_2$K$_D$A$_D$A products (r1, Scheme 1). Because this reaction proceeds via a loose transition state, the binding energy between the protonated vancomycin and the neutral peptide can be reasonably estimated by the difference in the total energy of the products (e.g., the protonated vancomycin and the neutral peptide) and the protonated vancomycin-peptide complex including the ZPE correction. However, low-energy structures of [V + H]$^+$ and Ac$_2$K$_D$A$_D$A are different from the structures of the corresponding species in the complex suggesting that both [V + H]$^+$ and Ac$_2$K$_D$A$_D$A undergo rearrangement once the complex dissociates. Because of the conformational flexibility of the peptide and the vancomycin it is not clear whether the conformational change occurs in the transition state or after
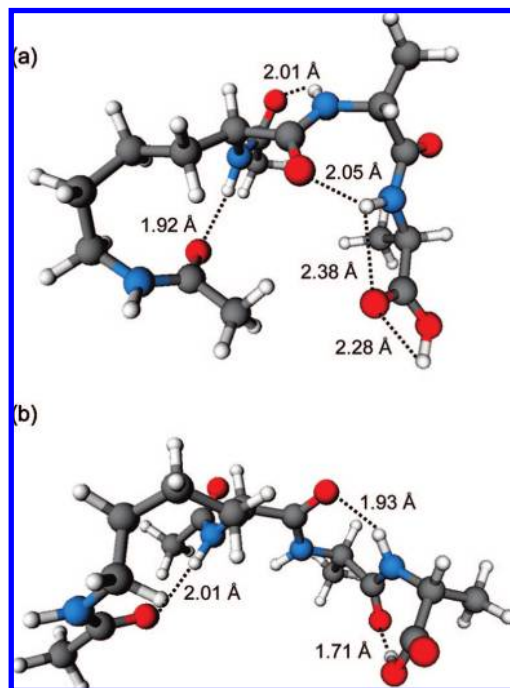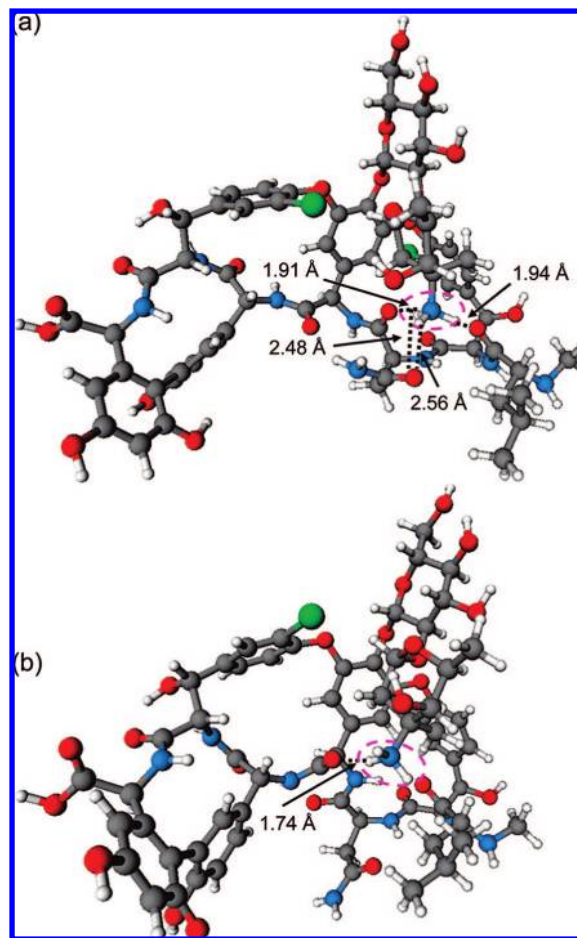
Figure 6. B3LYP/6−31G(d) optimized structures of neutral Ac_2KDADA in (a) folded and (b) extended conformations. The dotted lines indicate the hydrogen bonds.

the products separate from each other. In order to estimate the binding energy of $[V + Ac_2KDADA + H]^+$ based on the DFT calculations, we examined different possible conformations of the major reaction products.

Two types of conformations were considered for the neutral Ac_2KDADA. The lowest-energy conformation of the neutral peptide shown in Figure 6a has a folded structure stabilized by five short hydrogen bonds (1.92−2.38 Å) between carbonyl oxygens and -N2H, -N3H, and -N4H amide nitrogens. The second conformation considered as a possible structure of the neutral peptide in the transition state is shown in Figure 6b. This extended structure resembles the conformation of the peptide in the $[V + Ac_2KDADA + H]^+$ model complex, in which the amide (-N2H and -N4H) and the C-terminal carboxyl groups form three hydrogen bonds (1.71−2.01 Å) with carbonyl groups. The energy of this extended conformation obtained at the B3LYP/6−31G(d) level of theory is only 2.9 kcal/mol higher than the energy of the most stable folded structure shown in Figure 6(a).

Similarly, two types of conformations were considered for the $[V + H]^+$ protonated at the N_a site. The folded conformation shown in Figure 7a was initially adopted from the lowest energy structure obtained using MD simulations, and then optimized using the ONIOM (B3LYP/6−31G(d):B3LYP/3−21G) method. In this structure, protonated nitrogen of the disaccharide group (N_a) is solvated by four carbonyl groups of the vancomycin cage via four strong hydrogen bonds (1.91−2.56 Å). The asparagine side chain is folded into the vancomycin cage forming two short hydrogen bonds (2.48 and 2.56 Å) between the carbonyl group of the asparagine residue and the protonated N_a. The extended structure that resembles the $[V + H]^+$ conformation in the complex is shown in Figure 7b. This conformation was initially obtained from the most stable structure of the $[V + Ac_2KDADA + H]^+$ species and optimized using the ONIOM (B3LYP/6−31G(d):B3LYP/3−21G) method. In this structure the pro-

Figure 7. ONIOM(B3LYP/6−31G(d):B3LYP/3−21G) optimized structures of $[V + H]^+$ in (a) folded and (b) extended conformations. The dotted lines indicate the hydrogen bonds, and the pink dash encloses the protonation site.

tonated N_a is stabilized by one strong hydrogen bond (1.74 Å) with a carbonyl group of the vancomycin cage. The vancomycin cage in this conformation is more open because the asparagine side chain is not involved in solvation of the protonated N_a. It is interesting to note that although these two conformations are quite different, ONIOM (B3LYP/6−31G(d):B3LYP/3−21G) calculations suggest that the extended $[V + H]^+$ is only 2.8 kcal/mol less stable than the folded structure.

The uncertainty in the calculated binding energy originating from the conformational flexibility of the peptide and the vancomycin cage during fragmentation was estimated using relative energies of the folded and extended conformations of the major products (Ac_2KDADA and $[V + H]^+$) that determine the lower and upper limits of the vancomycin-Ac_2KDADA binding affinity, respectively. The resulting lower and upper limit estimates (including the ZPE correction obtained at the B3LYP/ 3−21G level of theory) of the binding energy between the protonated vancomycin and the neutral peptide are 36.3 and 42.0 kcal/mol, respectively, These values are in good agreement with the experimental binding energy of 30.9 ± 1.8 kcal/mol (Table 1).

5.5. Proton Affinities (PA). Protonated Ac_2KDADA is a minor reaction product formed via reaction r2 in Scheme 1. The branching ratio between $[V + H]^+$ and $[Ac_2KDADA + H]^+$ product ions can be used to estimate the relative proton affinity (PA) of the corresponding neutral species using the expression

Table 2. Comparison of the theoretical and experimental binding energies (kcal/mol) of vancomycin aglycon (VA) and vancomycin (V) with peptides (Ac$_D$A$_D$A and Ac$_2$K$_D$A$_D$A)

complex	theory				experiment	
	model system	E	E_0[b,c]	k_1[d]	k_2[d]	
VA-Ac$_D$A$_D$A	[VA + H]$^+$[Ac$_D$A$_D$A]	28.6[a]				
	[VA + H]$^+$[Ac$_D$A$_D$A − H]$^-$	122.7[a]				
V−Ac$_2$K$_D$A$_D$A	[V + Ac$_2$K$_D$A$_D$A + H]$^+$	46.7 (40.7)[b]	42.0 (36.3)	30.9 (±1.8)	30.5 (±1.8)	

[a] Obtained from the geometry optimization and single energy calculation at B3LYP/6−31G(d) level of theory. [b] The upper and lower limit (values in parentheses) of binding energies obtained using ONIOM (B3LYP/6−31G(d):B3LYP/3−21G) method. [c] Including the ZPE correction obtained at the B3LYP/3−21G level of theory. [d] Obtained from the RRKM modeling of the experimental data.

Table 3. Proton Affinities (PAs) of Ac$_2$K$_D$A$_D$A (N1, N2, N3, and N4) and Vancomycin (N$_a$ and N$_b$) at Various Positions Calculated by Using B3LYP with Various Basis Sets (kcal/mol)

basis sets	protonation sites					
	N1	N2	N3	N4	N$_a$	N$_b$
6−31G(d)//3−21G	234.2	219.9	215.0	210.1	272.1	262.5
	227.1[a]	212.2[a]	207.8[a]	203.3[a]		
6−31G(d)	237.6	222.0	215.2	212.8		
	229.2[b]	213.6[b]	207.2[b]	205.2[b]		
ONIOM(6−31G(d):3−21G)					269.1[43]	
					254.4[43c]	

[a] Including the zero-point energy (ZPE) correction obtained at the B3LYP/3−21G level of theory. [b] Including the zero-point energy (ZPE) correction obtained at the B3LYP/6−31G(d) level of theory. [c] Including the zero-point energy (ZPE) correction obtained at the ONIOM(B3LYP/6−31G(d):B3LYP/3−21G) method and level of theory.

of the kinetic method.[51] According to our experimental data the PA of the vancomycin is higher than the PA of the Ac$_2$K$_D$A$_D$A by 11 ± 4 kcal/mol, while the difference in entropy effects is 17 ± 3 e.u. It is interesting to compare this result with the relative PA obtained from DFT calculations.

Gas-phase PAs of four different protonation sites of the Ac$_2$K$_D$A$_D$A (Figure 2) calculated at the B3LYP/6−31G(d) level of theory are listed in Table 3. The calculated PA decreases in the order of PA(N1) > PA(N2) > PA(N3) > PA(N4), indicating that the secondary amine of the acetylated lysine side chain (N1) is the most basic protonation site of the Ac$_2$K$_D$A$_D$A with PA of 237.6 kcal/mol without the ZPE correction and 229.2 kcal/mol including the ZPE correction. Because N1 is the most basic site of the peptide ligand, the ground-state structure of [Ac$_2$K$_D$A$_D$A + H]$^+$ protonated at N$_1$ (not shown) most likely represents the conformation of the minor fragment ion ([Ac$_2$K$_D$A$_D$A + H]$^+$) observed in the experiment.

PAs of the two most basic protonation sites of vancomycin (N$_a$ and N$_b$, Figure 1) are listed in Table 3. The initial conformations of V and [V + H]$^+$ were adopted from the lowest-energy structures obtained using MD simulations. All the structures were optimized at the B3LYP/3−21G level of theory, and single-point energies were obtained at the B3LYP/6−31G(d) level of theory. The PA of the disaccharide group without the ZPE correction (N$_a$) (272.1 kcal/mol) is higher than the PA of *N*-methyl-leucine (N$_b$) (265.8 kcal/mol) by 6.3 kcal/mol suggesting that the most stable [V + H]$^+$ structure is protonated at the N$_a$ site. As discussed earlier, MD simulations suggest that protonation at the N$_a$ site is 40−43 kcal/mol more favorable than protonation at the N$_b$ site. It is interesting to note that while the relative energetics of the two protonation sites of vancomycin obtained from MD simulations is not accurate, the same trend in the relative stabilities of the different structures was obtained using MD simulations and DFT.

(51) (a) Cooks, R. G.; Kruger, T. L. *J. Am. Chem. Soc.* **1977**, *99*, 1279. (b) McLuckey, S. A.; Cameron, D.; Cooks, R. G. *J. Am. Chem. Soc.* **1981**, *103*, 1313. (c) Zheng, X.; Cooks, R. G. *J. Phys. Chem. A*, **2002**, *106*, 9939.

Subsequent optimizations and frequency calculations required to obtain the ZPE correction were performed for V and [V + H]$^+$ protonated at the N$_a$ site using ONIOM(B3LYP/6−31G(d): B3LYP/3−21G) method.[46] The PA of vancomycin of 254.4 kcal/mol including the ZPE correction (Table 3) was obtained at this level of theory. This value is 25.2 kcal/mol higher than the PA of Ac$_2$K$_D$A$_D$A (229.2 kcal/mol). However, the difference in the values of PAs (ΔPA) determined from the experimental data is only 11 ± 4 kcal/mol. The discrepancy between the theoretical and experimental data could be attributed to several factors. First, PAs of vancomycin and Ac$_2$K$_D$A$_D$A were obtained using different levels of theory: B3LYP/6−31G(d) for the peptide and ONIOM(B3LYP/6−31G(d):B3LYP/3−21G) for vancomycin. Second, the calculated values represent the PA at 0 K, while the experimental results were obtained at ca. 450 K. The difference between heats of formation at 0 and 450 K can be readily estimated using calculated vibrational frequencies of the neutral and protonated species. The value of ΔPA of 22.7 kcal/mol at 450 K was estimated based on the ΔPA at 0 K. This difference is still much larger than the experimentally determined ΔPA of 11 kcal/mol. Finally we note that theoretical PAs were derived from the ground-state energy of neutral and protonated species. However, it is likely that the structures of neutral and protonated species formed experimentally differ from the lowest-energy structures obtained from DFT calculations.

6. Discussion

6.1. Structures of [V + Ac$_2$K$_D$A$_D$A + H]$^+$. DFT calculations suggest that the most stable gas-phase structure of the [V + Ac$_2$K$_D$A$_D$A + H]$^+$ complex (Figure 5) is obtained when the canonical nonzwitterionic vancomycin protonated at the disaccharide group is bound to the neutral Ac$_2$K$_D$A$_D$A peptide molecule. In contrast, the most stable structures of both vancomycin and the vancomycin-Ac$_2$K$_D$A$_D$A complex in solution determined from NMR experiments are zwitterions, in which the N-termini of both vancomycin and peptide are protonated and the C-termini are deprotonated.[16–19] Zwitterionic

structures are stabilized in solution by efficient solvation of the protonated N-terminus and the deprotonated C-terminus of the vancomycin cage by the solvent molecules. However, zwitterionic structures are significantly destabilized in the absence of solvent. As a result, isolated amino acids and peptides commonly assume canonical structures in the gas phase.[52] Our results demonstrate that the structure of the singly protonated gas-phase V−Ac₂KDADA complex is significantly different from the solution phase structure.

6.2. Binding Energies. Previous computational studies carried out at the B3LYP/6−31G(d) level of theory showed that the interaction energy in the neutral complex of the vancomycin aglycon (VA) and the AcDADA peptide is 122.7 kcal/mol without the ZPE correction. The neutral ([VA + H]⁺[AcDADA − H]⁻) complex examined in that study was composed of the protonated VA ([VA + H]⁺) and the deprotonated AcDADA ([AcDADA − H]⁻).[31,32] Our calculations performed at the same level of theory (Table 2) are in excellent agreement with the previously reported value for the strength of this interaction. In contrast, the binding affinity between the protonated VA and the neutral AcDADA in the [VA + H]⁺[AcDADA] model complex is only 28.6 kcal/mol without the ZPE correction (Table 2).[53] It follows that the strong binding between the VA and the AcDADA reported by Lee et al.[31,32] mainly originates from the electrostatic interaction between [VA + H]⁺ and [AcDADA − H]⁻ that accounts for more than 90 kcal/mol of the binding energy. Because charge-induced dipole interaction is much weaker than the charge−charge interaction, the binding energy of the [VA + H]⁺[AcDADA] complex is much lower, and interaction energy between the VA cage and the peptide ligand is mainly determined by the intermolecular hydrogen bonding. Interestingly, the calculated binding energy of the [V + Ac₂KDADA + H]⁺ complex of 40.7−46.7 kcal/mol (without the ZPE correction) is much higher than the binding energy obtained for the more simple [VA + H]⁺[AcDADA] model system. The higher binding energy of this complex is attributed to the direct participation of the ionizing proton located on the disaccharide group of vancomycin in the intermolecular hydrogen bonding.

As discussed earlier, the theoretical values of the binding energy of the vancomycin-peptide complex were obtained from the difference in the energy of the reactant ([V + Ac₂KDADA + H]⁺) and the major products ([V + H]⁺ and Ac₂KDADA) including the ZPE correction. Due to the limited computational resources, only the lowest energy conformation of the reactant ([V + Ac₂KDADA + H]⁺) and of the product ion, [V + H]⁺, were selected from MD simulations for further DFT optimization. Although it is possible that these structures are not at the global minimum of the potential energy surface we believe that

they adequately represent the most populated family of conformations sampled in our experiments conducted at 450 K.

The complexity of the V−Ac₂KDADA system and the conformational flexibility of the resulting products introduce a significant uncertainty into the calculated binding energy. In this study we estimated this uncertainty using two different pairs of structures of the major products—the most stable folded structures that represent the products at infinite separation and extended/open structures that resemble the structures of the vancomycin and the peptide in the complex. These two pairs of structures were used to estimate the lower and the upper limit of the binding energy. The uncertainty in the calculated binding energy introduced by the conformational flexibility of the products is 5.7 kcal/mol. The resulting theoretical binding energy between the protonated vancomycin and the neutral peptide is in the range of 36.3−42.0 kcal/mol—in good agreement with the experimental result (30.9 ± 1.8 kcal/mol).

Another possible source of uncertainty originates from the accuracy of the calculated ZPE correction to the binding energy. The ZPE correction was derived from the frequency calculations of the reactant ([V + Ac₂KDADA + H]⁺) and the major products ([V + H]⁺ and Ac₂KDADA) that were performed at different levels of theory. However, the uncertainty in the ZPE correction should be rather small. For example, ZPEs of the folded Ac₂KDADA structure obtained at the B3LYP/3−21G and B3LYP/6−31G(d) levels of theory are 288.7 and 287.5 kcal/mol, respectively. The difference of 1.2 kcal/mol between the values of the ZPE obtained at different levels of theory is small compared to the uncertainty in the determination of absolute energies of the lowest-energy structures using DFT calculations. It follows that the uncertainty in the ZPE correction is rather small and should not significantly affect the conclusions.

6.3. Activation Entropy (ΔS‡). The activation entropy is another important factor that determines the rate of dissociation of gas-phase ions. Our previous studies suggested that entropy is the major driving force in dissociation of large biomolecules in the gas phase.[26,54] Very high positive values of activation entropies were obtained from the RRKM modeling of the experimental SID data for both dissociation pathways of the V−Ac₂KDADA complex (Table 1) suggesting that both r1 and r2 are entropy-driven pathways. The corresponding preexponential factors of 5.5 × 10³⁰ s⁻¹ and 9.4 × 10²⁶ s⁻¹ were derived from the activation entropies of r1 and r2, respectively, at 450 K. These values are similar to the values reported for dissociation of protein−ligand complexes using blackbody infrared radiative dissociation (BIRD).[55] However, to the best of our knowledge pre-exponential factors of this magnitude have never been reported for much smaller systems such as the V−Ac₂KDADA complex studied in this work. It has been suggested that large pre-exponential factors originate from breaking of multiple interactions and softening of numerous vibrational modes during dissociation of protein−ligand complexes in the gas phase.[55] Dissociation of the noncovalent complex examined in our experiments is also associated with breaking of multiple intermolecular hydrogen bonds between the vancomycin cage and the peptide and loosening of the vibrational modes constrained by the binding. Finally we note that the difference in activation entropies of 17.2 e.u. obtained experimentally is in excellent agreement with the 22 e.u. difference in the protonation entropies of the vancomycin and

(52) (a) Wyttenbach, T.; Bushnell, J. E.; Bowers, M. T. *J. Am. Chem. Soc.* **1998**, *120*, 5098. (b) Toroz, D.; van Mourik, T. *Mol. Phys.* **2007**, *105*, 209. (c) Chapo, C. J.; Paul, J. B.; Provencal, R. A.; Roth, K.; Saykally, R. J. *J. Am. Chem. Soc.* **1998**, *120*, 12956. (d) Reva, I. D.; Plokhotnichenko, A. M.; Stepanian, S. G.; Ivanov, A. Yu.; Radchenko, E. D.; Sheina, G. G.; Blagoi, Y. P. *Chem. Phys. Lett.* **1995**, *232*, 141. (e) Locke, M. J.; McIver, R. T. *J. Am. Chem. Soc.* **1983**, *105*, 4226. (f) Lemoff, A. S.; Bush, M. F.; O'Brien, J. T.; Williams, E. R. *J. Phys. Chem. A* **2006**, *110*, 8433. (g) Jockusch, R. A.; Lemoff, A. S.; Williams, E. R. *J. Phys. Chem. A* **2001**, *105*, 10929.
(53) The lowest energy conformation of AcDADA has an extended structure that is very similar to the structure of the ligand in the complex. Consequently, the binding affinity of vancomycin-AcDADA model system was determined using the calculated energy of the extended conformation.

(54) Laskin, J.; Futrell, J. H. *J. Phys. Chem. A* **2003**, *107*, 5836.
(55) Felitsyn, N.; Kitova, E. N.; Klassen, J. S. *Anal. Chem.* **2001**, *73*, 4647.

the peptide ligand estimated based on the calculated vibrational frequencies of the corresponding neutral and protonated species.

7. Summary

Time- and energy-resolved SID experiments have been extensively used to study the energetics and dynamics of dissociation of covalent bonds in gas-phase peptide ions.[26–28] In this work we used this technique for the first time for quantitative investigation of the energetics of noncovalent interactions in the gas phase. SID of the singly protonated vancomycin-Ac_2KDADA complex was used to determine the binding affinity between vancomycin antibiotic and the cell-wall analogue peptide. Gas-phase fragmentation of this complex is dominated by the formation of the protonated vancomycin and the neutral peptide. The protonated Ac_2KDADA formed via a competing dissociation channel is observed as a minor product ion. The energetics and dynamics of the competing dissociation pathways were determined using the RRKM modeling of the experimental data. We found that entropy plays a major role in determining the dissociation rate of the $V-Ac_2KDADA$ complex. DFT calculations were used to obtain the optimized geometries, energies, and vibrational frequencies of vancomycin, peptide, and several model complexes. Computational results indicate that the PA of vancomycin is higher than the PA of the Ac_2KDADA, which rationalizes the predominant formation of the $[V + H]^+$ fragment ion.

Calculated binding affinities were obtained for several model systems. Comparison between the experimental data and theoretical calculations suggest that the singly protonated $V-Ac_2KDADA$ complex is composed of the neutral peptide and protonated vancomycin. The binding energy of 30.9 ± 1.8 kcal/mol obtained from the experimental data is in good agreement with the theoretical value of $36.3-42.0$ kcal/mol obtained for the model system, in which the vancomycin is protonated at the disaccharide group. This study demonstrates that the combination of time- and energy-resolved SID experiments and DFT calculations provides a unique insight on the structures and stabilities of large noncovalent complexes.

Supporting Information Available: Complete refs 44 and 45. Geometries of B3LYP/6−31G(d) optimized structures of peptide (Ac_2KDADA, $[Ac_2KDADA + H]^+$, $AcDADA$) and $[VA + H]^+[AcDADA]$ model complex. Geometries of ONIOM(B3LYP/6−31G(d):B3LYP/3−21G) optimized structures of vancomycin (V, $[V + H]^+$) and vancomycin-peptide complexes ($[V + Ac_2KDADA + H]^+$). This material is available free of charge *via* the Internet at http://pubs.acs.org. Other information is also available upon request.

JA802643G